

VideoMAE: Masked Autoencoders are Data-Efficient Learners for Self-Supervised Video Pre-Training

Zhan Tong^{1,2*} Yibing Song² Jue Wang² Limin Wang¹

tongzhan@smail.nju.edu.cn {yibingsong.cv, arphid}@gmail.com lmwang@nju.edu.cn

Abstract

Pre-training video transformers on extra large-scale datasets is generally required to achieve premier performance on relatively small datasets. In this paper, we show that video masked autoencoders (VideoMAE) are data-efficient learners for self-supervised video pre-training (SSVP). We are inspired by the recent ImageMAE (He et al., 2021) and propose customized video tube masking with an extremely high ratio. This simple design makes video reconstruction a more challenging self-supervision task, thus encouraging extracting more effective video representations during this pre-training process. We obtain three important findings on SSVP: (1) An extremely high proportion of masking ratio (i.e., 90% to 95%) still yields favorable performance of VideoMAE. The temporally redundant video content enables a higher masking ratio than that of images. (2) VideoMAE achieves impressive results on very small datasets (i.e., around 3k-4k videos) without using any extra data. (3) VideoMAE shows that data quality is more important than data quantity for SSVP. Domain shift between pre-training and target datasets is an important issue. Notably, our VideoMAE with the vanilla ViT can achieve 85.8% on Kinetics-400, 75.3% on Something-Something V2, 90.8% on UCF101, and 61.1% on HMDB51, without using any extra data. Code is available at <https://github.com/MCG-NJU/VideoMAE>.

1. Introduction

Transformer (Vaswani et al., 2017) has brought significant progress in natural language processing (Devlin et al., 2019;

* Work is done during internship at Tencent AI Lab. ¹State Key Laboratory for Novel Software Technology, Nanjing University ²Tencent AI Lab. Correspondence to: Limin Wang <lmwang@nju.edu.cn>.

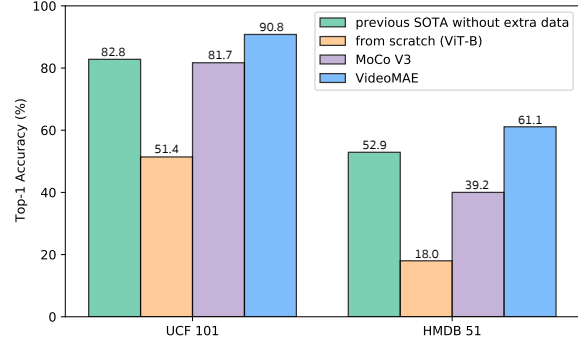


Figure 1. VideoMAE is a **data-efficient learner** that allows to effectively train video transformers only from limited video data (e.g., 9.5k clips in UCF101, and 3.5k clips in HMDB51) without any ImageNet pre-training. VideoMAE significantly outperforms training from scratch, MoCo v3 pre-training (Chen et al., 2021b), and the previous best performance (Diba et al., 2021) without extra data on these small-scale video datasets.

Brown et al., 2020; Radford et al., 2018). The vision transformer (Dosovitskiy et al., 2021) also improves a series of computer vision tasks including image classification (Touvron et al., 2021; Zhou et al., 2021), object detection (Carion et al., 2020; Liu et al., 2021a), semantic segmentation (Xie et al., 2021), object tracking (Cui et al., 2022), and video recognition (Bertasius et al., 2021; Arnab et al., 2021). The multi-head self-attention upon linearly projected visual tokens is capable of modeling global dependency among visual content either spatially or temporally. The inductive bias is effectively reduced via this flexible attention mechanism.

Training effective vision transformers (ViTs) typically necessitates large-scale supervised datasets. Initially, the pre-trained ViTs achieve favorable performance by using hundreds of millions of labeled images (Dosovitskiy et al., 2021). For video transformers (Arnab et al., 2021; Bertasius et al., 2021), they are usually derived from image-based transformers and heavily depend on the pre-trained models from large-scale image data (e.g., ImageNet (Russakovsky et al., 2015)). Previous trials (Arnab et al., 2021; Bertasius et al., 2021) on training video transformers from scratch yield unsatisfied results (except for MViT (Fan et al., 2021) with a strong inductive bias). Therefore, the learned video transformers are naturally biased by image-based models,

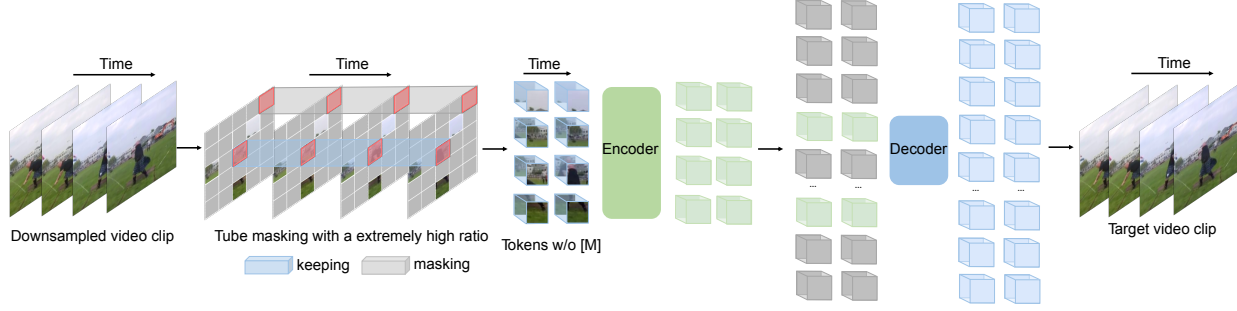


Figure 2. Our VideoMAE Architecture. Our VideoMAE performs the task of masking random cubes and reconstructing the missing ones with an asymmetric encoder-decoder architecture. Due to high redundancy and temporal correlation in videos, we present the customized design of tube masking with an extremely high ratio (90% to 95%). This simple design enables us to create a more challenging and meaningful self-supervised task to make the learned representations capture more useful spatiotemporal structures.

and it still remains a challenge that *how to effectively and efficiently train a vanilla vision transformer on the video dataset itself without using any pre-trained model or extra image data*. Moreover, the existing video datasets are relatively small compared with image datasets, which further increases the difficulty of training video transformers from scratch. Meanwhile, self-supervised learning has shown remarkable performance by using large-scale image datasets (Chen et al., 2021b; Caron et al., 2021). The learned representations have outperformed the ones via supervised learning when being transferred to downstream tasks. It is expected that this self-supervised learning paradigm can provide a promising solution to address the challenge of training video transformers.

Following the success of masked autoencoding in NLP (Devlin et al., 2019) and images (He et al., 2021; Bao et al., 2021), we present a new self-supervised video pre-training (SSVP) method, termed as *Video Masked Autoencoder* (VideoMAE). Our VideoMAE inherits the simple pipeline of masking random cubes and reconstructing the missing ones. However, the extra time dimension of videos makes them different from images in this masked modeling. First, video frames are often densely captured, and their semantics varies slowly in time (Zhang & Tao, 2012). This temporal redundancy would increase the risk of recovering missing pixels from the spatiotemporal neighborhood with little high-level understanding. Furthermore, video could be viewed as the temporal evolution of static appearance, and there exists a correspondence between frames. This temporal correlation could lead to information leakage (i.e., masked spatiotemporal content re-occurrence) during reconstruction unless a specific masking strategy is considered. In this sense, for each masked cube, it is easy to find a corresponding and unmasked copy in adjacent frames. This property would make the learned models identify some “shortcut” features that are hard to generalize to new scenarios.

To make video masked modeling more effective, in this paper, we present a customized design of tube masking with an extremely high ratio in our VideoMAE. First, due to tem-

poral redundancy, we use an *extremely high* masking ratio to drop the cubes from the downsampled clips. This simple strategy not only effectively increases the pre-training performance but also greatly reduces the computational cost due to the asymmetric encoder-decoder architecture. Second, to consider temporal correlation, we devise a simple yet effective *tube masking* strategy, which turns out to be helpful in relieving the risk of information leakage for cubes with no or negligible motion during reconstruction. With this simple yet effective design in our VideoMAE, we are able to successfully train vanilla ViT backbones on the relatively small-scale video datasets such as Something-Something (Goyal et al., 2017), UCF101 (Soomro et al., 2012), and HMDB51 (Kuehne et al., 2011), which significantly outperform the previous state of the art under the setting without extra data. In summary, the main contribution of this paper is threefold:

- To our best knowledge, we present the first masked video autoencoder that performs well for SSVP on relatively small-scale video datasets. To relieve the information leakage issue in the video reconstruction task, we present a simple design of tube masking with an extremely high ratio, which turns out to be effective in improving the performance of VideoMAE.
- Aligned with the results in NLP and Images on masked modeling, our VideoMAE demonstrates that this simple masking and reconstruction strategy provides a good solution to self-supervised video pre-training. The models pre-trained with our VideoMAE significantly outperform those trained from scratch or pre-trained with contrastive learning methods.
- We obtain extra important finds on masked modeling that might be ignored in the previous research in NLP and Images. (1) Our results demonstrate that VideoMAE is a data-efficient learner that could be successfully trained with only 3.5k videos. (2) VideoMAE shows that data quality is more important than quantity for SSVP when a domain shift exists between the source and target dataset.

2. Related Work

Video representation learning. Learning good video representations has been heavily investigated in the literature. The supervised learning methods (Wang et al., 2019; Tran et al., 2018; Feichtenhofer et al., 2019; Feichtenhofer, 2020; Bertasius et al., 2021) usually depend on the image backbones. The video encoder backbones are first pre-trained with image data in a supervised form. Then, these backbones are fine-tuned on the video dataset for classifying human actions. Besides supervised learning, semi-supervised video representation learning is also studied (Singh et al., 2021). The representations of labeled training samples are utilized to generate supervision signals for unlabeled ones. Supervised or semi-supervised representation learning mainly uses a top-down training paradigm, which is not effective in exploring the inherent video data structure itself.

For self-supervised learning, the prior knowledge of temporal information has been widely exploited to design pretext tasks (Wang & Gupta, 2015; Misra et al., 2016; Xu et al., 2019; Benaim et al., 2020) for SSVP. Recently, contrastive learning (Han et al., 2020b; Pan et al., 2021b; Han et al., 2020a; Qian et al., 2021a) is popular to learn better video representation. However these methods heavily rely on strong data augmentation and large batch size (Feichtenhofer et al., 2021). Predicting the video clip with autoencoders in pixel space has been explored for representation learning (Patraucean et al., 2015; Srivastava et al., 2015) by using CNN or LSTM backbones or video generation with autoregressive GPT (Yan et al., 2021). Our VideoMAE aims to use the simple masked autoencoder with recent ViT backbones to perform data-efficient SSVP. Our VideoMAE provides a conceptually simple yet effective alternative to contrastive learning for SSVP and brings several vital findings on transformer-based SSVP as we will present.

Masked visual modeling. Masked visual autoencoder has been proposed to learn effective visual representations based on the simple pipeline of masking and reconstruction. These works mainly focus on the image domain. The early work (Vincent et al., 2010) treated the masking and a noise type in denoised autoencoders (Vincent et al., 2008) or inpainted missing regions with context (Pathak et al., 2016) by using convolutions. Recently, masked visual autoencoder used Transformer backbones for masking and reconstruction. iGPT (Chen et al., 2020b) followed the success of GPT (Brown et al., 2020; Radford et al., 2019) in NLP and operated a sequence of pixels for prediction. The original ViT (Dosovitskiy et al., 2021) investigated the masked token prediction for self-supervised pre-training. More recently, the success of vision transformer has led to investigation of Transformer-based architectures for masked visual modeling (Bao et al., 2021; Dong et al., 2021; He et al., 2021; Wei et al., 2021; Xie et al., 2022; Zhou et al., 2022).

BEiT (Bao et al., 2021) and BEVT (Wang et al., 2021b) followed BERT (Devlin et al., 2019) and proposed to learn visual representations from images and videos by predicting the discrete tokens (Ramesh et al., 2021). ImageMAE (He et al., 2021) introduced an asymmetric encoder-decoder architecture for masked image modeling. MaskFeat (Wei et al., 2021) proposed to reconstruct the features of masked tokens to perform self-supervised pre-training in videos.

Our VideoMAE is inspired by the ImageMAE and introduces specific designs for SSVP. Our work differs from recent video masked modeling methods in several aspects. 1) *Prediction target*. Our VideoMAE performs pre-training by directly predicting the normalized cube pixels, while BEVT and MaskFeat predict the discrete tokens from pre-trained VQ-VAE and HOG features, respectively. 2) *Computational efficiency*. Our VideoMAE only needs to feed the unmasked tokens (e.g., 10%) into the encoder in self-supervised learning. BEVT and MaskFeat put all tokens into the encoder during the pre-training phase. 3) *Backbone*. Our VideoMAE uses the plain ViT, while the Swin and MViT in BEVT and MaskFeat are with multi-scale and hierarchical architectures. 4) *Prediction head*. Our VideoMAE generates the target by a shallow Transformer decoder, while BEVT and MaskFeat all use two-layer MLP as the target head. Overall, our VideoMAE enjoys a simpler design for the whole pipeline, obtaining higher efficiency and slightly better accuracy.

3. Proposed Method

In this section, we first revisit ImageMAE (He et al., 2021). Then we analyze the characteristics of video data. Finally, we show how we explore MAE in the video data by presenting our VideoMAE.

3.1. Revisiting Masked Autoencoders

ImageMAE (He et al., 2021) performs the masking and reconstruction task with an asymmetric encoder-decoder architecture. The input image $I \in \mathcal{R}^{3 \times H \times W}$ is first divided into regular non-overlapping patches of size 16×16 , and each patch is represented with *token embedding*. Then a subset of tokens are randomly masked with a high masking ratio (75%), and only the remaining ones are fed into the transformer *encoder* Φ_{enc} . Finally, a shallow *decoder* Φ_{dec} is placed on top of the visible tokens from the encoder and learnable mask tokens to reconstruct the image. The *loss function* is mean squared error (MSE) loss between the normalized masked tokens and reconstructed ones in the pixel space:

$$\mathcal{L} = \frac{1}{\Omega} \sum_{p \in \Omega} |I(p) - \hat{I}(p)|^2, \quad (1)$$

where p is the token index, Ω is the set of masked tokens, I is the input image, and \hat{I} is the reconstructed one.

3.2. Characteristics of Video Data

Compared with static images, video data contain temporal relations. We show the motivation of our VideoMAE by analyzing video characteristics.

Temporal redundancy. There are frequently captured frames in a video. The semantics vary slowly in the temporal dimension (Zhang & Tao, 2012). We observe that consecutive frames are highly redundant, as shown in Figure 3. This property leads to two critical issues in masked video autoencoding. First, it would be less efficient to keep the original temporal frame rate for pre-training. This would draw us to focus more on static or slow motions in our masked modeling. Second, temporal redundancy greatly dilutes motion representations. This would make the task of reconstructing missing pixels not difficult under the normal masking ratio (e.g., 50% to 75%). The encoder backbone is not effective in capturing motion representations.

Temporal correlation. Videos could be viewed as the temporal extension of static appearance, and therefore there exists an inherent correspondence between adjacent frames. This temporal correlation could increase the risk of information leakage in the masking and reconstruction pipeline. In this sense, as shown in Figure 3, we can reconstruct the masked patches by finding the spatiotemporal corresponding unmasked patches in the adjacent frames under plain random masking or frame masking. In this case, it might guide the VideoMAE to learn low-level temporal correspondence rather than high-level information such as spatiotemporal reasoning over the content. To alleviate this behavior, we need to propose a new masking strategy to make the reconstruction more challenging and encourage effective learning of spatiotemporal structure representations.

3.3. VideoMAE

To relieve the above issues in video masked modeling, we make the customized design in our VideoMAE. The overall pipeline is shown in Figure 2. Our VideoMAE takes the *downsampled frames* as inputs and uses the *cube embedding* to obtain video tokens. Then, we propose a simple design of *tube masking with high ratio* to perform video pre-training with an asymmetric encoder-decoder architecture. We adopt the vanilla ViT with *joint space-time attention* as backbone.

Temporal downsampling. According to the above analysis on temporal redundancy over consecutive frames, we propose to use the strided temporal sampling strategy to perform more efficient video pre-training. Formally, one video clip consisting of t consecutive frames is first randomly sampled from the original video V . We then use temporal sampling to compress the clip to T frames, each of which contains $H \times W \times 3$ pixels. In experiments, the stride τ is set to 4 and 2 on Kinetics and Something-Something.

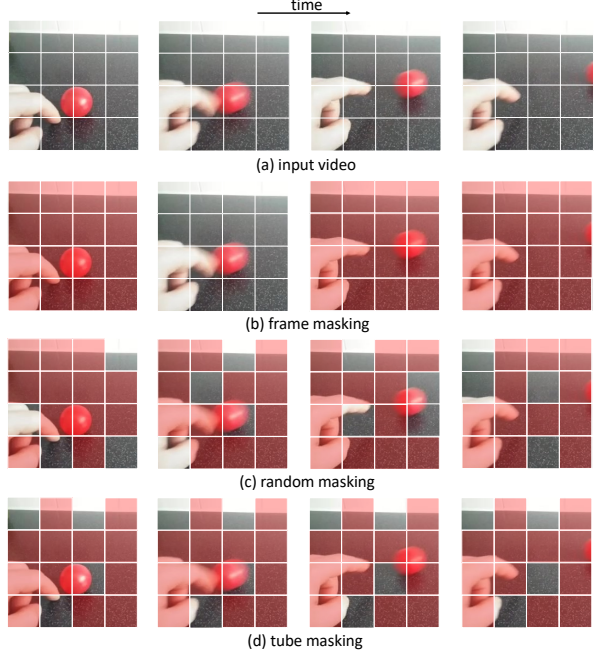


Figure 3. Slowness is a general prior in (a) input video data (Zhang & Tao, 2012). This leads to two important characteristics in time: temporal redundancy and temporal correlation. Temporal redundancy makes it possible to recover the pixel under an extremely high masking ratio. Temporal correlation leads us to easily reconstruct the missing pixel by finding those corresponding patches in adjacent frames under plain (b) frame masking or (c) random masking. To avoid this simple task and encourage learning representative representation, we propose a (d) tube masking, where the masking map is the same for all frames.

Cube embedding. We adopt the joint space-time cube embedding (Arnab et al., 2021; Fan et al., 2021) in our VideoMAE, where we treat each cube of size $2 \times 16 \times 16$ as one token embedding. Thus, the cube embedding layer obtains $\frac{T}{2} \times \frac{H}{16} \times \frac{W}{16}$ 3D tokens and maps each token to the channel dimension D . This design can decrease the spatial and temporal dimension of input, which helps to alleviate the spatiotemporal redundancy in videos.

Tube masking with extremely high ratio. First, temporal redundancy is a factor affecting VideoMAE design. We find that VideoMAE is in favor of extremely high masking ratios (e.g. 90% to 95%) compared with the ImageMAE. Video information density is much lower than images, and we expect a high ratio to increase the reconstruction difficulty. This high masking ratio is helpful to mitigate the information leakage during masked modeling and make masked video reconstruction a meaningful self-supervised pre-training task.

Second, temporal correlation is another factor in our VideoMAE design. Even under the extremely high masking ratio, we can still improve the masking efficiency by proposing the temporal tube masking mechanism. Temporal tube masking enforces a mask to expand over the whole temporal

VideoMAE: Masked Autoencoders are Data-Efficient Learners for Self-Supervised Video Pre-Training

blocks	top-1	top-5	GPU mem.
1	68.2	91.7	7.9G
2	68.9	92.1	10.2G
4	69.3	92.3	14.7G
8	69.0	92.1	23.7G

(a) **Decoder depth.** 4 blocks of decoder achieve the best accuracy and efficiency trade-off. “GPU mem.” is GPU memory during pre-training, benchmarked in one GPU with a batch size of 16.

case	top-1	top-5
from scratch	32.6	61.9
ImageNet-21k sup.	61.4	86.6
IN-21k+K400 sup.	64.8	89.8
VideoMAE	69.3	92.3

(d) **Pre-training strategy.** Our VideoMAE works the best without using any extra data. “sup.” is supervised training.

case	ratio	top-1	top-5
tube	75	67.3	91.5
tube	90	69.3	92.3
random	90	68.3	91.8
frame	87.5*	61.5	87.6

(b) **Mask sampling.** We compare different masking strategies. Our proposed tube masking with an extremely high ratio works the best. *“87.5” means masking 14/16 frames.

dataset	method	top-1	top-5
IN-1K	ImageMAE	64.5	89.5
K400	VideoMAE	68.2	91.6
SSV2	VideoMAE	69.3	92.3

(e) **Pre-training dataset.** Our VideoMAE works best when directly pre-training on Something-Something V2.

input	target	top-1	top-5
16×2	center	62.7	88.4
16×1	16×1	53.2	80.6
16×2	16×2	69.3	92.3
16×2	32×1	69.0	92.0

(c) **Reconstruction target.** $T \times \tau$ denotes frames \times stride. *center* denotes the center frame of the input clip. 16×2 subsampled video frames as reconstruction targets are effective and best.

case	top-1	top-5
L1 loss	68.8	92.1
MSE loss	69.3	92.3
Smooth L1 loss	68.6	92.1

(f) **Loss function.** MSE loss works the best for the masking and reconstruction task in VideoMAE.

Table 1. Ablation experiments on **Something-Something V2**. Our backbone is 16-frame ViT-B described in Appendix A and all models are pre-trained with *mask ratio* $\rho=90\%$ for 800 epochs. We use the fine-tuning setting for evaluation and report the top-1/top-5 accuracy. All models share the same inference protocol, i.e., 2 clips \times 3 crops. Default choice for our model is colored in gray.

axis, namely, different frames sharing the same masking map. Mathematically, the tube mask mechanism can be expressed as $\mathbb{I}[p_{x,y,\cdot} \in \Omega] \sim \text{Bernoulli}(\rho_{\text{mask}})$ and different time t shares the same value. With this mechanism, temporal neighbors of masked cubes are always masked. So for some cubes with no or small motion (e.g., finger cube in 4th row of Figure 3 (d)), we can not find the spatiotemporal corresponding content in all frames. In this way, it would encourage our VideoMAE to reason over high-level semantics to recover these totally missing cubes. This simple strategy can alleviate the information leakage for cubes with no or negligible motion and turns out to be effective in practice for masked video pre-training.

Backbone: joint space-time attention. Due to the high proportion of masking ratio mentioned above, only a few tokens are left as the input for the encoder. To better capture high-level spatio-temporal information in the remaining tokens, we use the vanilla ViT backbone (Dosovitskiy et al., 2021) and adopt the joint space-time attention (Arnab et al., 2021). Thus, all pair tokens could interact with each other in the multi-head self-attention layer. The specific architecture design for the encoder and decoder is shown in Appendix A. The quadratic complexity of the joint space-time attention mechanism is a computational bottleneck, while our design of an extremely high masking ratio alleviates this issue by only putting the unmasked tokens (e.g., 10%) into the encoder during the pre-training phase.

4. Experiments

4.1. Datasets

We evaluate our VideoMAE on five common video datasets: Kinetics-400 (Kay et al., 2017), Something-Something

V2 (Goyal et al., 2017), UCF101 (Soomro et al., 2012), HMDB51 (Kuehne et al., 2011) and AVA (Gu et al., 2018). The Kinetics-400 contains around 240k training videos and 20k validation videos of 10s from 400 classes. The Something-Something V2 is a relatively large-scale video dataset, having around 169k videos for training and 20k videos for validation. In contrast to Kinetics-400, this dataset contains 174 motion-centric action classes. These two large-scale video datasets focus on different visual cues for action recognition. UCF101 and HMDB51 are two relatively small and old video datasets, which contain around 9.5k/3.5k train/val videos and 3.5k/1.5k train/val videos, respectively. Compared with those large-scale video datasets, these two small datasets are more suitable to verify the effectiveness of VideoMAE, as training large ViT models is more challenging on small datasets. Moreover, we also transfer the learned VideoMAE to downstream task. For action detection, we work on AVA, a dataset proposed for spatiotemporal localization of human actions with 211k training and 57k validation video segments. In experiments, we strictly follow the default setting on these datasets by pre-training VideoMAE on the training set and reporting the top-1 accuracy on the validation set. The implementation details of VideoMAE are described in Appendix B.

4.2. Ablation Studies

In this subsection, we perform in-depth ablation studies of VideoMAE with the default 16-frame ViT-B on Something-Something V2. The specific architecture design for the encoder and decoder is shown in Appendix A. For these evaluations, we use the fine-tuning setting, and all models share the same inference protocol, i.e., 2 clips \times 3 crops.

Decoder design. The lightweight decoder is one key component in our VideoMAE. We conduct experiments with the different depths in Table 1a. Unlike in ImageMAE, a deep decoder here is important for better performance, while a shallow decoder could reduce the GPU memory consumption. We take 4 blocks for the decoder by default. The decoder width is set to half channel of the encoder (e.g., 384-d for ViT-B), following the empirical design in the image domain.

Masking strategy. We compare different masking strategies in Table 1b. When increasing the masking ratio from 75% to 90% for tube masking, the performance boosts from 67.3% to 69.3%. Then, with an extremely high ratio, we find tube masking also achieves better performance than plain random masking and frame masking. We attribute these interesting observations to the redundancy and temporal correlation in videos. We argue that our default designs enforce the networks to capture more useful spatiotemporal structures and therefore make VideoMAE a more challenging task, which a good self-supervised learner hunger for.

Reconstruction target. First, if we only employ the center frame in the video clip as the target, the results would decrease greatly. The sampling stride is also sensitive. The result of consecutive 16 frames is significantly lower than our default downsampled clip (53.2% v.s. 69.3%). We also try to reconstruct the consecutive 32 frames from the downsampled 16 frames, but it obtains slightly worse results.

Pre-training strategy. We compare different pre-training strategies in Table 1d. Similar to previous trials (Arnab et al., 2021; Bertasius et al., 2021), training video transformers from scratch yields unsatisfied results on this motion-sensitive dataset. When pre-trained on the large-scale image dataset (ImageNet-21K), the video transformer obtains better accuracy from 32.6% to 61.4%. Using the models pre-trained on both ImageNet-21K and Kinetics further increases accuracy to 64.8%. Our VideoMAE can effectively train a video transformer from the video itself without using any extra data and achieve the best performance 69.3%.

Pre-training dataset. First, we pre-train the ViT-B on ImageNet-1K for 1600 epochs, following the recipes in (He et al., 2021). Then we inflate the 2D patch embedding layer to our cube embedding layer following (Carreira & Zisserman, 2017) and fine-tune the model on the Something-Something dataset. This result surpasses the model trained *from scratch* as shown in Table 1e. We also compare this ImageMAE pre-trained model with the VideoMAE model pre-trained on Kinetics. We see that our VideoMAE model can achieve better performance than ImageMAE. However, these two pre-trained models fail to yield better performance than our VideoMAE only pre-trained on the Something-Something dataset. We argue that domain shift between pre-training and target datasets could be an important issue.

dataset	training data	<i>from scratch</i>	MoCo v3	VideoMAE
K400	240k	68.8	74.2	79.4
Sth-Sth V2	169k	32.6	54.2	69.3
UCF101	9.5k	51.4	81.7	90.8
HMDB51	3.5k	18.0	39.2	61.1

Table 2. Comparisons with the results of previous **self-supervised pre-training methods** on different datasets. We take 16-frame ViT-B as the default backbone. Notably, here MoCo v3 and VideoMAE all only use the *unlabelled* data in the training set of each dataset for pre-training and are all fine-tuned for evaluation.

method	epoch	ft. acc.	lin. acc.	hours	speedup
MoCo v3	300	54.2	33.7	61.7	-
VideoMAE	800	69.3	38.9	19.5	3.2 ×

Table 3. Comparisons with the **efficiency and effectiveness** on Something-Something V2. We report the fine-tuning (ft) and linear probing (lin) accuracy (%). The **wall-clock time** of pre-training is benchmarked in 64 Tesla V100 GPUs with PyTorch.

method	K400 → SSV2	K400 → UCF	K400 → HMDB
MoCo v3	62.4	93.2	67.9
VideoMAE	68.2	96.1	73.3

Table 4. Comparisons with the **feature transferability** on smaller datasets. We take 16-frame ViT-B as the default backbone. Notably, here MoCo v3 and VideoMAE are all pre-trained on Kinetics-400 with *unlabelled* data in the training set. Then the pre-trained model is fine-tuned on target datasets for evaluation.

Loss function. Table 1f contains an ablation study of loss function. We find that the MSE loss could achieve a higher result compared with the L1 loss and smooth L1 loss. Therefore, we employ the MSE loss by default.

4.3. Main Results and Analysis

VideoMAE: data-efficient learner. The self-supervised video pre-training (SSVP) has been extensively studied in previous works, but they mainly use the CNN-based backbones. Few works have investigated transformer-based backbone in SSVP. Therefore, to demonstrate the effectiveness of VideoMAE for transformer-based SSVP, we compare with two methods implemented by ourselves: (1) training from scratch, (2) pre-training with contrastive learning (MoCo v3 (Chen et al., 2021b)). For training from scratch, we carefully tune these hyper-parameters to successfully pre-train ViT-Base from the training set of dataset. For pre-training with MoCo v3, we strictly follow the training practice in its image counterpart and carefully avoid the collapse issue.

The recognition accuracy is reported in Table 2. We see that our VideoMAE significantly outperforms the other two training methods. For instance, on the largest dataset of Kinetics-400, our VideoMAE outperforms training from scratch by around 10% and MoCo v3 pre-training by around 5%. This superior performance demonstrates that masked autoencoder provides an effective pre-training mechanism for video transformers. We also see that the performance gap

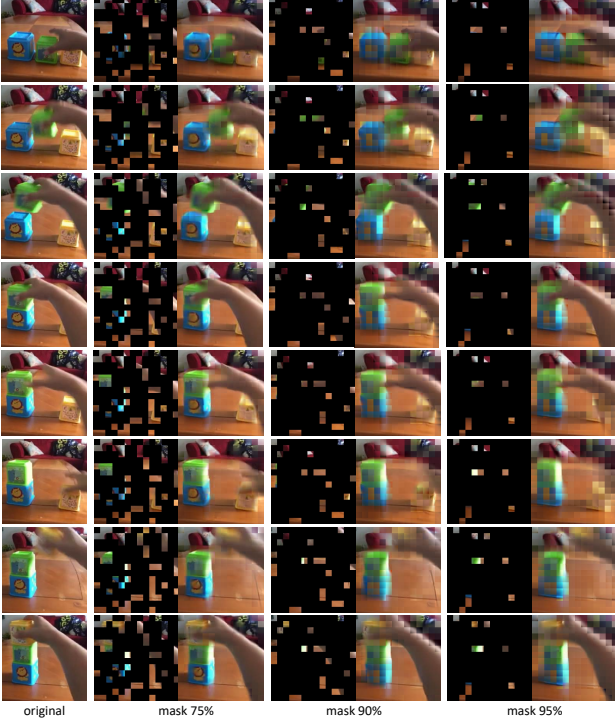


Figure 4. Reconstruction results of Something-Something V2 validation video using the VideoMAE pre-trained with a masking ratio of 90%. More examples of visualization are shown in Appendix D.

between our VideoMAE and the other two methods becomes larger as the training set becomes smaller. Notably, even with only 3.5k training clips on HMDB51, our VideoMAE pre-training can still obtain a satisfying accuracy (around 61%). This new result demonstrates that VideoMAE is a more data-efficient learner for SSVP. This property is particularly important for scenarios with limited data available and different with contrastive learning methods.

We compare the efficiency of VideoMAE pre-training and MoCo v3 pre-training in Table 3. The task of masked autoencoding with a high ratio is more challenging and thereby requires more training epochs (800 vs. 300). Thanks to the asymmetric encoder-decoder in our VideoMAE and extremely high masking ratio, our pre-training time is much shorter than MoCo v3 (19.5 vs. 61.7 hours).

High masking ratio. In VideoMAE, one core design is the extremely high masking ratio. We perform an investigation of this design on the Kinetics-400 and Something-Something V2 datasets. The results are shown in Figure 5. We see that the best masking ratio is extremely high, and even 95% can achieve good performance for both datasets. This result is difference from BERT (Devlin et al., 2019) in NLP and MAE (He et al., 2021) in images. We analyze the temporal redundancy and correlation in videos makes it possible for our VideoMAE to learn plausible outputs with such a high masking ratio.

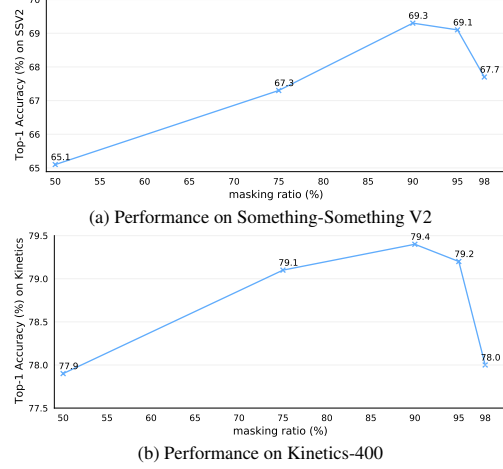


Figure 5. The effect of **masking ratio** on (a) Something-Something V2 and (b) Kinetics-400. Our default backbone is 16-frame ViT-B described in Appendix A. The results show that a extremely high masking ratio (90%) achieves the best efficiency and effectiveness trade-off on both video datasets.

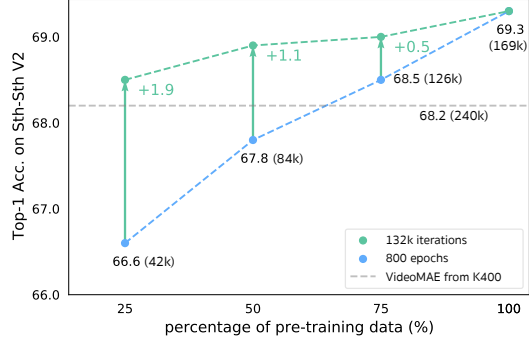


Figure 6. **Data efficiency** of VideoMAE representations. Our default backbone is 16-frame ViT-B described in Appendix A. • denotes that all models are trained for the **same** 132k iterations, and • denotes that all models are trained for the **same** 800 epochs. Note that it takes 132k iterations to pre-train the model for 800 epochs on the full training set of Something-Something V2.

We also visualize the reconstructed examples in Figure 4. We see that even under a high masking ratio, VideoMAE can produce satisfying reconstructed results. This implies that our VideoMAE is able to learn useful representations that capture the holistic spatiotemporal structure in videos.

Transfer learning: quality vs. quantity. To further investigate the generalization ability of VideoMAE in representation learning, we transfer the learned VideoMAE from Kinetics-400 to Something-Something V2, UCF101, and HMDB51. The results are shown in Table 4, and we compare them with the MoCo v3 pre-training method. The models pre-trained by our VideoMAE are better than those pre-trained by MoCo v3, demonstrating that our VideoMAE learns more transferable representations.

Comparing Table 2 and Table 4, the transferred represen-

Method	Architecture	Pre-train Dataset	Extra Labels	$T \times \tau$	GFLOPs	Param	mAP
supervised (Feichtenhofer et al., 2021)	SlowOnly-R50	Kinetics-400	✓	8×8	42	32	22.2
supervised (Fan et al., 2021)	MViTv1-B	Kinetics-400	✓	16×4	71	36	24.5
supervised (Fan et al., 2021)	MViTv1-B	Kinetics-400	✓	64×3	455	36	27.3
supervised (Feichtenhofer, 2020)	X3D-XL	Kinetics-600	✓	16×5	48	11	27.4
supervised (Fan et al., 2021)	MViTv1-B	Kinetics-600	✓	16×4	71	36	26.1
supervised (Fan et al., 2021)	MViTv1-B-24	Kinetics-600	✓	32×3	236	53	28.7
supervised (Tang et al., 2020)	AIA	Kinetics-600	✓	8×8+32×2	N/A	N/A	32.3
supervised (Pan et al., 2021a)	ACAR-Net	Kinetics-700	✓	8×8+32×2	N/A	N/A	33.3
CVRL (Qian et al., 2021b)	SlowOnly-R50	Kinetics-400	✗	32×2	42	32	16.3
ρ BYOL $_{\rho=3}$ (Feichtenhofer et al., 2021)	SlowOnly-R50	Kinetics-400	✗	8×8	42	32	23.4
ρ MoCo $_{\rho=3}$ (Feichtenhofer et al., 2021)	SlowOnly-R50	Kinetics-400	✗	8×8	42	32	20.3
MaskFeat \uparrow 312 (Wei et al., 2021)	MViT-L	Kinetics-400	✓	40×3	2828	218	37.5
MaskFeat \uparrow 312 (Wei et al., 2021)	MViT-L	Kinetics-600	✓	40×3	2828	218	38.8
VideoMAE(Ours)	ViT-B	Kinetics-400	✗	16×4	180	87	26.7
VideoMAE(Ours)	ViT-B	Kinetics-400	✓	16×4	180	87	31.8
VideoMAE(Ours)	ViT-L	Kinetics-400	✗	16×4	597	305	34.3
VideoMAE(Ours)	ViT-L	Kinetics-400	✓	16×4	597	305	37.8
VideoMAE(Ours)	ViT-L	Kinetics-700	✗	16×4	597	305	36.1
VideoMAE(Ours)	ViT-L	Kinetics-700	✓	16×4	597	305	39.3

Table 5. Comparison with the state-of-the-art methods on AVA v2.2. We report the mean Average Precision (mAP) on validation set. “Extra labels \times ” means only *unlabelled* data is used during the pre-training phase and the pre-trained models are directly transferred to the downstream dataset. “Extra labels \checkmark ” means the pre-trained models are additionally fine-tuned on the pre-training dataset with *labels* before transferred to the downstream dataset. $T \times \tau$ refers to frame number and corresponding sample rate. “N/A” indicates the numbers are not available for us.

Method	Backbone	Extra data	Extra labels	Frames	GFLOPs	Param	Top-1	Top-5
TSM $_{En}$ (Lin et al., 2019)	ResNet50 $\times 2$		✓	16+16	130 \times 2 \times 3	49	66.0	90.5
TANet $_{En}$ (Liu et al., 2021c)	ResNet50 $\times 2$	ImageNet-1K	✓	8+16	99 \times 2 \times 3	51	66.0	90.1
TDN $_{En}$ (Wang et al., 2021a)	ResNet101 $\times 2$		✓	8+16	198 \times 1 \times 3	88	69.6	92.2
SlowFast (Feichtenhofer et al., 2019)	ResNet101		✓	8+32	106 \times 1 \times 3	53	63.1	87.6
MViTv1 (Fan et al., 2021)	MViTv1-B	Kinetics-400	✓	64	455 \times 1 \times 3	37	67.7	90.9
TimeSformer (Bertasius et al., 2021)	ViT-B		✓	8	196 \times 1 \times 3	121	59.5	N/A
TimeSformer (Bertasius et al., 2021)	ViT-L	ImageNet-21K	✓	64	5549 \times 1 \times 3	430	62.4	N/A
ViViT FE (Arnab et al., 2021)	ViT-L		✓	32	995 \times 4 \times 3	N/A	65.9	89.9
Motionformer (Patrick et al., 2021b)	ViT-B		✓	16	370 \times 1 \times 3	109	66.5	90.1
Motionformer (Patrick et al., 2021b)	ViT-L	IN-21K+K400	✓	32	1185 \times 1 \times 3	382	68.1	91.2
Video Swin (Liu et al., 2021b)	Swin-B		✓	32	321 \times 1 \times 3	88	69.6	92.7
BEVT (Wang et al., 2021b)	Swin-B	IN-1K+K400+DALLE	✗	32	321 \times 1 \times 3	88	70.6	N/A
MaskFeat \uparrow 312 (Wei et al., 2021)	MViT-L	Kinetics-600	✓	40	2828 \times 1 \times 3	218	75.0	95.0
VideoMAE$_{\rho=90\%}$(Ours)	ViT-B		✗	16	180 \times 2 \times 3	87	70.6	92.7
VideoMAE$_{\rho=90\%}$(Ours)	ViT-L	no external data	✗	16	597 \times 2 \times 3	305	74.2	94.7
VideoMAE$_{\rho=90\%}$(Ours)	ViT-L		✗	32	1436 \times 1 \times 3	305	75.3	95.2

Table 6. Comparison with the state-of-the-art methods on Something-Something V2. Our VideoMAE $_{\rho=90\%}$ reconstructs normalized cube pixels and is pre-trained for 2400 epochs. “Extra labels \times ” means only *unlabelled* data is used during the pre-training phase. “N/A” indicates the numbers are not available for us.

tation outperforms the original VideoMAE models trained from its own dataset on UCF101 and HMDB51. In contrast, the transferred representation is worse on Something-Something V2. To figure out whether this inconsistent result is caused by the large scale of Something-Something V2, we further perform a detailed investigation by decreasing the pre-training video numbers. In this study, we run two experiments: (1) pre-training with the same epochs, and (2) pre-training with the same time budget. The result is shown in Figure 6. We see that more training iterations

could contribute to better performance when we decrease the size of the pre-training set. Surprisingly, even with only 42k pre-training videos, we can still obtain better accuracy than the K400 pre-trained models with 240k videos (68.5% vs. 68.2%). This result implies that domain shift is another important factor, and data quality is more important than data quantity in SSVP when there exists a difference between pre-training and target datasets. It also demonstrates that VideoMAE is a data-efficient learner for SSVP.

Method	Backbone	Extra data	Extra labels	Frames	GFLOPs	Param	Top-1	Top-5
NL I3D (Wang et al., 2018)	ResNet101	ImageNet-1K	✓	128	359×10×3	62	77.3	93.3
TANet (Liu et al., 2021c)	ResNet152		✓	16	242×4×3	59	79.3	94.1
TDN _{En} (Wang et al., 2021a)	ResNet101 _{×2}		✓	8+16	198×10×3	88	79.4	94.4
Video Swin (Liu et al., 2021b)	Swin-B		✓	32	282×4×3	88	80.6	94.6
TimeSformer (Bertasius et al., 2021)	ViT-B	ImageNet-21K	✓	8	196×1×3	121	78.3	93.7
TimeSformer (Bertasius et al., 2021)	ViT-L		✓	96	8353×1×3	430	80.7	94.7
ViViT FE (Arnab et al., 2021)	ViT-L		✓	128	3980×1×3	N/A	81.7	93.8
Motionformer (Patrick et al., 2021b)	ViT-B		✓	16	370×10×3	109	79.7	94.2
Motionformer (Patrick et al., 2021b)	ViT-L		✓	32	1185×10×3	382	80.2	94.8
Video Swin (Liu et al., 2021b)	Swin-L		✓	32	604×4×3	197	83.1	95.9
ViViT FE (Arnab et al., 2021)	ViT-L	JFT-300M	✓	128	3980×1×3	N/A	83.5	94.3
ViViT (Arnab et al., 2021)	ViT-H	JFT-300M	✓	32	3981×4×3	N/A	84.9	95.8
VIMPAC (Tan et al., 2021)	ViT-L	HowTo100M+DALLE	✗	10	N/A×10×3	307	77.4	N/A
BEVT (Wang et al., 2021b)	Swin-B	IN-1K+DALLE	✗	32	282×4×3	88	80.6	N/A
MaskFeat \uparrow 352 (Wei et al., 2021)	MViT-L	Kinetics-600	✗	40	3790×4×3	218	87.0	97.4
ip-CSN (Tran et al., 2019)	ResNet152	no external data	✗	32	109×10×3	33	77.8	92.8
SlowFast (Feichtenhofer et al., 2019)	R101+NL		✗	16+64	234×10×3	60	79.8	93.9
MViTv1 (Fan et al., 2021)	MViTv1-B		✗	32	170×5×1	37	80.2	94.4
MaskFeat (Wei et al., 2021)	MViT-L		✗	16	377×10×1	218	84.3	96.3
VideoMAE$_{\rho=90\%}$(Ours)	ViT-B	no external data	✗	16	180×5×3	87	80.9	94.7
VideoMAE$_{\rho=90\%}$(Ours)	ViT-L		✗	16	597×5×3	305	84.7	96.5
VideoMAE\uparrow320$_{\rho=90\%}$(Ours)	ViT-L		✗	32	3958×5×3	305	85.8	97.1

Table 7. Comparison with the state-of-the-art methods on Kinetics-400. Our VideoMAE $_{\rho=90\%}$ reconstructs normalized cube pixels. Here models are self-supervised pre-trained for 1600 epochs on Kinetics-400. “Extra labels ✗” means only *unlabelled* data is used during the pre-training phase. “N/A” indicates the numbers are not available for us.

Transfer learning: downstream action detection. We also transfer the learned VideoMAE on Kinetics-400 to downstream action detection dataset AVA. Following the standard setting (Gu et al., 2018), we evaluate on top 60 common classes with mean Average Precision (mAP) as the metric under IoU threshold of 0.5. The results are shown in the Table 5. After self-supervised pre-training on Kinetics-400, our VideoMAE with the vanilla ViT-L can achieve 34.3 mAP on AVA, which demonstrates the strong transferability of our VideoMAE. If the pre-trained ViT-L is additionally fine-tuned on Kinetics-400, the transfer learning performance can further increase to 37.8 mAP. This result surpasses 37.5 mAP of MaskFeat, which needs more input frames and higher spatial resolution. More remarkably, when we pre-train VideoMAE (ViT-Large) on the larger Kinetics-700 dataset for 800 epochs, we finally obtain 39.3 mAP on the downstream AVA dataset. These results demonstrate that the self-supervised pre-trained models transfer well not only on classification task but on more complex action detection task.

Comparison with the state of the art. We compare with the previous state-of-the-art performance on the Kinetics-400 and Something-Something V2 datasets. The results are reported in Table 6 and Table 7. Our VideoMAE can easily scale up with more powerful backbones (ViT-Large), more frames (32), and higher input resolution (320). Our VideoMAE achieves the top-1 accuracy of 75.3% on Something-Something V2 and 85.8% on Kinetics-400 without using any extra data. Videos in the Something-Something V2

dataset focus on the motion property instead of objects or scene context. We see that the existing state-of-the-art methods on Something-Something V2 all depend on the external data for pre-training. In the contrary, our VideoMAE (ViT-L) without any external data significantly outperforms previous best results by around 5%. On Kinetics-400, our VideoMAE the vanilla ViT backbone can obtain better performance than those transformer-based methods, such as TimeSformer (Bertasius et al., 2021), ViViT (Arnab et al., 2021), Motionformer (Patrick et al., 2021b), Video Swin (Liu et al., 2021b) and MViT (Fan et al., 2021). Our VideoMAE \uparrow 320 (ViT-L) also achieves superior performance compared to the ViViT-H, which is supervised pre-trained on JFT-300M (85.8% vs. 84.9% in Top-1 and 97.1% vs. 95.8% in Top-5).

5. Conclusion

In this paper, we have presented a simple and data-efficient self-supervised learning method (VideoMAE) for video transformer pre-training. Our VideoMAE introduces two critical designs of extremely high masking ratio and tube masking strategy to make the video reconstruction task more challenging. This harder task would encourage VideoMAE to learn more useful features and relieve the information leakage issue. Empirical results demonstrate this simple algorithm works well for video datasets of different scales. In particular, we are able to learn effective VideoMAE only with thousands of video clips, which has significant practical value for scenarios with limited data available.

References

Alayrac, J.-B., Recasens, A., Schneider, R., Arandjelovic, R., Ramapuram, J., De Fauw, J., Smaira, L., Dieleman, S., and Zisserman, A. Self-supervised multimodal versatile networks. In *Advances in Neural Information Processing Systems*, 2020.

Alwassel, H., Mahajan, D., Korbar, B., Torresani, L., Ghanem, B., and Tran, D. Self-supervised learning by cross-modal audio-video clustering. In *Advances in Neural Information Processing Systems*, 2020.

Arnab, A., Dehghani, M., Heigold, G., Sun, C., Lučić, M., and Schmid, C. Vivit: A video vision transformer. In *IEEE/CVF International Conference on Computer Vision*, 2021.

Bao, H., Dong, L., and Wei, F. BEiT: BERT pre-training of image transformers. *arXiv preprint arXiv:2106.08254*, 2021.

Benaim, S., Ephrat, A., Lang, O., Mosseri, I., Freeman, W. T., Rubinstein, M., Irani, M., and Dekel, T. Speednet: Learning the speediness in videos. In *IEEE/CVF Conference on Computer Vision and Pattern Recognition*, 2020.

Bertasius, G., Wang, H., and Torresani, L. Is space-time attention all you need for video understanding? In *International Conference on Machine Learning*, 2021.

Brown, T., Mann, B., Ryder, N., Subbiah, M., Kaplan, J. D., Dhariwal, P., Neelakantan, A., Shyam, P., Sastry, G., Askell, A., Agarwal, S., Herbert-Voss, A., Krueger, G., Henighan, T., Child, R., Ramesh, A., Ziegler, D., Wu, J., Winter, C., Hesse, C., Chen, M., Sigler, E., Litwin, M., Gray, S., Chess, B., Clark, J., Berner, C., McCandlish, S., Radford, A., Sutskever, I., and Amodei, D. Language models are few-shot learners. In *Advances in Neural Information Processing Systems*, 2020.

Carion, N., Massa, F., Synnaeve, G., Usunier, N., Kirillov, A., and Zagoruyko, S. End-to-end object detection with transformers. In *European Conference on Computer Vision*, 2020.

Caron, M., Touvron, H., Misra, I., Jégou, H., Mairal, J., Bojanowski, P., and Joulin, A. Emerging properties in self-supervised vision transformers. In *IEEE/CVF International Conference on Computer Vision*, 2021.

Carreira, J. and Zisserman, A. Quo vadis, action recognition? A new model and the kinetics dataset. In *IEEE/CVF Conference on Computer Vision and Pattern Recognition*, 2017.

Chen, M., Radford, A., Child, R., Wu, J., Jun, H., Luan, D., and Sutskever, I. Generative pretraining from pixels. In *International Conference on Machine Learning*, 2020a.

Chen, M., Radford, A., Child, R., Wu, J., Jun, H., Luan, D., and Sutskever, I. Generative pretraining from pixels. In *International Conference on Machine Learning*, 2020b.

Chen, P., Huang, D., He, D., Long, X., Zeng, R., Wen, S., Tan, M., and Gan, C. Rspnet: Relative speed perception for unsupervised video representation learning. In *Proceedings of the AAAI Conference on Artificial Intelligence*, 2021a.

Chen, X., Xie, S., and He, K. An empirical study of training self-supervised vision transformers. In *IEEE/CVF International Conference on Computer Vision*, 2021b.

Cubuk, E. D., Zoph, B., Shlens, J., and Le, Q. V. Randaugment: Practical automated data augmentation with a reduced search space. In *Proceedings of the IEEE/CVF Conference on Computer Vision and Pattern Recognition Workshops*, 2020.

Cui, Y., Jiang, C., Wang, L., and Wu, G. Mixformer: End-to-end tracking with iterative mixed attention. In *CVPR*, 2022.

Devlin, J., Chang, M.-W., Lee, K., and Toutanova, K. Bert: Pre-training of deep bidirectional transformers for language understanding. In *North American Chapter of the Association for Computational Linguistics*, 2019.

Diba, A., Sharma, V., Safdari, R., Lotfi, D., Sarfraz, S., Stiefelhagen, R., and Van Gool, L. Vi2clr: Video and image for visual contrastive learning of representation. In *IEEE/CVF International Conference on Computer Vision*, 2021.

Dong, X., Bao, J., Zhang, T., Chen, D., Zhang, W., Yuan, L., Chen, D., Wen, F., and Yu, N. Poco: Perceptual codebook for bert pre-training of vision transformers. *arXiv preprint arXiv:2111.12710*, 2021.

Dosovitskiy, A., Beyer, L., Kolesnikov, A., Weissenborn, D., Zhai, X., Unterthiner, T., Dehghani, M., Minderer, M., Heigold, G., Gelly, S., et al. An image is worth 16x16 words: Transformers for image recognition at scale. In *International Conference on Learning Representations*, 2021.

Fan, H., Xiong, B., Mangalam, K., Li, Y., Yan, Z., Malik, J., and Feichtenhofer, C. Multiscale vision transformers. In *IEEE/CVF International Conference on Computer Vision*, 2021.

Feichtenhofer, C. X3d: Expanding architectures for efficient video recognition. In *IEEE/CVF Conference on Computer Vision and Pattern Recognition*, 2020.

Feichtenhofer, C., Fan, H., Malik, J., and He, K. Slowfast networks for video recognition. In *IEEE/CVF International Conference on Computer Vision*, 2019.

Feichtenhofer, C., Fan, H., Xiong, B., Girshick, R., and He, K. A large-scale study on unsupervised spatiotemporal representation learning. In *IEEE/CVF Conference on Computer Vision and Pattern Recognition*, 2021.

Ghadiyaram, D., Tran, D., and Mahajan, D. Large-scale weakly-supervised pre-training for video action recognition. In *IEEE/CVF Conference on Computer Vision and Pattern Recognition*, 2019.

Goyal, R., Kahou, S. E., Michalski, V., Materzynska, J., Westphal, S., Kim, H., Haenel, V., Fründ, I., Yianilos, P., Mueller-Freitag, M., Hoppe, F., Thurau, C., Bax, I., and Memisevic, R. The "something something" video database for learning and evaluating visual common sense. In *IEEE/CVF International Conference on Computer Vision*, 2017.

Gu, C., Sun, C., Ross, D. A., Vondrick, C., Pantofaru, C., Li, Y., Vijayanarasimhan, S., Toderici, G., Ricco, S., Sukthankar, R., et al. Ava: A video dataset of spatiotemporally localized atomic visual actions. In *IEEE/CVF Conference on Computer Vision and Pattern Recognition*, 2018.

Han, T., Xie, W., and Zisserman, A. Self-supervised co-training for video representation learning. In *Advances in Neural Information Processing Systems*, 2020a.

Han, T., Xie, W., and Zisserman, A. Memory-augmented dense predictive coding for video representation learning. In *European Conference on Computer Vision*, 2020b.

He, K., Chen, X., Xie, S., Li, Y., Dollár, P., and Girshick, R. Masked autoencoders are scalable vision learners. *arXiv preprint arXiv:2111.06377*, 2021.

Hoffer, E., Ben-Nun, T., Hubara, I., Giladi, N., Hoefler, T., and Soudry, D. Augment your batch: Improving generalization through instance repetition. In *IEEE/CVF Conference on Computer Vision and Pattern Recognition*, 2020.

Hu, K., Shao, J., Liu, Y., Raj, B., Savvides, M., and Shen, Z. Contrast and order representations for video self-supervised learning. In *IEEE/CVF International Conference on Computer Vision*, 2021.

Kay, W., Carreira, J., Simonyan, K., Zhang, B., Hillier, C., Vijayanarasimhan, S., Viola, F., Green, T., Back, T., Natsev, P., Suleyman, M., and Zisserman, A. The kinetics human action video dataset. *arXiv preprint arXiv:1705.06950*, 2017.

Kondratyuk, D., Yuan, L., Li, Y., Zhang, L., Tan, M., Brown, M., and Gong, B. Movinets: Mobile video networks for efficient video recognition. In *IEEE/CVF Conference on Computer Vision and Pattern Recognition*, 2021.

Kuehne, H., Jhuang, H., Garrote, E., Poggio, T., and Serre, T. Hmdb: a large video database for human motion recognition. In *IEEE/CVF International Conference on Computer Vision*, 2011.

Lee, H., Huang, J., Singh, M., and Yang, M. Unsupervised representation learning by sorting sequence. In *IEEE/CVF International Conference on Computer Vision*, 2017.

Lin, J., Gan, C., and Han, S. TSM: temporal shift module for efficient video understanding. In *IEEE/CVF International Conference on Computer Vision*, 2019.

Liu, Z., Luo, D., Wang, Y., Wang, L., Tai, Y., Wang, C., Li, J., Huang, F., and Lu, T. Teinet: Towards an efficient architecture for video recognition. In *Proceedings of the AAAI Conference on Artificial Intelligence*, 2020.

Liu, Z., Lin, Y., Cao, Y., Hu, H., Wei, Y., Zhang, Z., Lin, S., and Guo, B. Swin transformer: Hierarchical vision transformer using shifted windows. In *IEEE/CVF International Conference on Computer Vision*, 2021a.

Liu, Z., Ning, J., Cao, Y., Wei, Y., Zhang, Z., Lin, S., and Hu, H. Video swin transformer. *arXiv preprint arXiv:2106.13230*, 2021b.

Liu, Z., Wang, L., Wu, W., Qian, C., and Lu, T. Tam: Temporal adaptive module for video recognition. In *IEEE/CVF International Conference on Computer Vision*, 2021c.

Loshchilov, I. and Hutter, F. Sgdr: Stochastic gradient descent with warm restarts. *arXiv preprint arXiv:1608.03983*, 2016.

Miech, A., Alayrac, J.-B., Smaira, L., Laptev, I., Sivic, J., and Zisserman, A. End-to-End Learning of Visual Representations from Uncurated Instructional Videos. In *IEEE/CVF Conference on Computer Vision and Pattern Recognition*, 2020.

Misra, I., Zitnick, C. L., and Hebert, M. Shuffle and learn: unsupervised learning using temporal order verification. In *European Conference on Computer Vision*, 2016.

Pan, J., Chen, S., Shou, M. Z., Liu, Y., Shao, J., and Li, H. Actor-context-actor relation network for spatio-temporal action localization. In *IEEE/CVF Conference on Computer Vision and Pattern Recognition*, 2021a.

Pan, T., Song, Y., Yang, T., Jiang, W., and Liu, W. Video-moco: Contrastive video representation learning with

temporally adversarial examples. In *IEEE/CVF Conference on Computer Vision and Pattern Recognition*, 2021b.

Paszke, A., Gross, S., Massa, F., Lerer, A., Bradbury, J., Chanan, G., Killeen, T., Lin, Z., Gimelshein, N., Antiga, L., Desmaison, A., Kopf, A., Yang, E., DeVito, Z., Raison, M., Tejani, A., Chilamkurthy, S., Steiner, B., Fang, L., Bai, J., and Chintala, S. Pytorch: An imperative style, high-performance deep learning library. In Wallach, H., Larochelle, H., Beygelzimer, A., d'Alché-Buc, F., Fox, E., and Garnett, R. (eds.), *Advances in Neural Information Processing Systems*, 2019.

Pathak, D., Krähenbühl, P., Donahue, J., Darrell, T., and Efros, A. A. Context encoders: Feature learning by inpainting. In *IEEE/CVF Conference on Computer Vision and Pattern Recognition*, 2016.

Patraucean, V., Handa, A., and Cipolla, R. Spatio-temporal video autoencoder with differentiable memory. *arXiv preprint arXiv:1511.06309*, 2015.

Patrick, M., Asano, Y. M., Kuznetsova, P., Fong, R., Henriques, J. F., Zweig, G., and Vedaldi, A. Multi-modal self-supervision from generalized data transformations. In *IEEE/CVF International Conference on Computer Vision*, 2021a.

Patrick, M., Campbell, D., Asano, Y. M., Metze, I. M. F., Feichtenhofer, C., Vedaldi, A., and Henriques, J. F. Keeping your eye on the ball: Trajectory attention in video transformers. In *Advances in Neural Information Processing Systems*, 2021b.

Piergiovanni, A., Angelova, A., and Ryoo, M. S. Evolving losses for unsupervised video representation learning. In *IEEE/CVF Conference on Computer Vision and Pattern Recognition*, 2020.

Qian, R., Meng, T., Gong, B., Yang, M.-H., Wang, H., Belongie, S., and Cui, Y. Spatiotemporal contrastive video representation learning. In *IEEE/CVF Conference on Computer Vision and Pattern Recognition*, 2021a.

Qian, R., Meng, T., Gong, B., Yang, M.-H., Wang, H., Belongie, S. J., and Cui, Y. Spatiotemporal contrastive video representation learning. In *IEEE/CVF Conference on Computer Vision and Pattern Recognition*, 2021b.

Radford, A., Narasimhan, K., Salimans, T., and Sutskever, I. Improving language understanding by generative pre-training. *OpenAI blog*, 2018.

Radford, A., Wu, J., Child, R., Luan, D., Amodei, D., and Sutskever, I. Language models are unsupervised multitask learners. *OpenAI blog*, 2019.

Ramesh, A., Pavlov, M., Goh, G., Gray, S., Voss, C., Radford, A., Chen, M., and Sutskever, I. Zero-shot text-to-image generation. In *International Conference on Machine Learning*, 2021.

Russakovsky, O., Deng, J., Su, H., Krause, J., Satheesh, S., Ma, S., Huang, Z., Karpathy, A., Khosla, A., Bernstein, M., et al. Imagenet large scale visual recognition challenge. *International Journal of Computer Vision*, 2015.

Singh, A., Chakraborty, O., Varshney, A., Panda, R., Feris, R., Saenko, K., and Das, A. Semi-supervised action recognition with temporal contrastive learning. In *IEEE/CVF Conference on Computer Vision and Pattern Recognition*, 2021.

Soomro, K., Zamir, A. R., and Shah, M. Ucf101: A dataset of 101 human actions classes from videos in the wild. *arXiv preprint arXiv:1212.0402*, 2012.

Srivastava, N., Mansimov, E., and Salakhutdinov, R. Unsupervised learning of video representations using lstms. *International Conference on Machine Learning*, 2015.

Szegedy, C., Vanhoucke, V., Ioffe, S., Shlens, J., and Wojna, Z. Rethinking the inception architecture for computer vision. In *IEEE/CVF Conference on Computer Vision and Pattern Recognition*, 2016.

Tan, H., Lei, J., Wolf, T., and Bansal, M. Vimpac: Video pre-training via masked token prediction and contrastive learning. *arXiv preprint arXiv:2106.11250*, 2021.

Tang, J., Xia, J., Mu, X., Pang, B., and Lu, C. Asynchronous interaction aggregation for action detection. In *European Conference on Computer Vision*, 2020.

Touvron, H., Cord, M., Douze, M., Massa, F., Sablayrolles, A., and Jégou, H. Training data-efficient image transformers & distillation through attention. In *International Conference on Machine Learning*, 2021.

Tran, D., Wang, H., Torresani, L., Ray, J., LeCun, Y., and Paluri, M. A closer look at spatiotemporal convolutions for action recognition. In *IEEE/CVF Conference on Computer Vision and Pattern Recognition*, 2018.

Tran, D., Wang, H., Feiszli, M., and Torresani, L. Video classification with channel-separated convolutional networks. In *IEEE/CVF International Conference on Computer Vision*, 2019.

Vaswani, A., Shazeer, N., Parmar, N., Uszkoreit, J., Jones, L., Gomez, A. N., Kaiser, Ł., and Polosukhin, I. Attention is all you need. In *Advances in Neural Information Processing Systems*, 2017.

Vincent, P., Larochelle, H., Bengio, Y., and Manzagol, P. Extracting and composing robust features with denoising autoencoders. In *International Conference on Machine Learning*, 2008.

Vincent, P., Larochelle, H., Lajoie, I., Bengio, Y., and Manzagol, P. Stacked denoising autoencoders: Learning useful representations in a deep network with a local denoising criterion. *Journal of Machine Learning Research*, 2010.

Wang, H., Tran, D., Torresani, L., and Feiszli, M. Video modeling with correlation networks. In *IEEE/CVF Conference on Computer Vision and Pattern Recognition*, 2020a.

Wang, J., Jiao, J., and Liu, Y.-H. Self-supervised video representation learning by pace prediction. In *European Conference on Computer Vision*, 2020b.

Wang, L., Xiong, Y., Wang, Z., Qiao, Y., Lin, D., Tang, X., and Gool, L. V. Temporal segment networks for action recognition in videos. *IEEE Transactions on Pattern Analysis and Machine Intelligence*, 2019.

Wang, L., Tong, Z., Ji, B., and Wu, G. TDN: Temporal difference networks for efficient action recognition. In *IEEE/CVF Conference on Computer Vision and Pattern Recognition*, 2021a.

Wang, R., Chen, D., Wu, Z., Chen, Y., Dai, X., Liu, M., Jiang, Y., Zhou, L., and Yuan, L. BEVT: BERT pretraining of video transformers. *arXiv preprint arXiv:2112.01529*, 2021b.

Wang, X. and Gupta, A. Unsupervised learning of visual representations using videos. In *IEEE/CVF International Conference on Computer Vision*, 2015.

Wang, X., Girshick, R., Gupta, A., and He, K. Non-local neural networks. In *IEEE/CVF Conference on Computer Vision and Pattern Recognition*, 2018.

Wei, C., Fan, H., Xie, S., Wu, C.-Y., Yuille, A., and Feichtenhofer, C. Masked feature prediction for self-supervised visual pre-training. *arXiv preprint arXiv:2112.09133*, 2021.

Xie, E., Wang, W., Yu, Z., Anandkumar, A., Alvarez, J. M., and Luo, P. Segformer: Simple and efficient design for semantic segmentation with transformers. In *Advances in Neural Information Processing Systems*, 2021.

Xie, Z., Zhang, Z., Cao, Y., Lin, Y., Bao, J., Yao, Z., Dai, Q., and Hu, H. Simmim: A simple framework for masked image modeling. In *International Conference on Computer Vision and Pattern Recognition (CVPR)*, 2022.

Xu, D., Xiao, J., Zhao, Z., Shao, J., Xie, D., and Zhuang, Y. Self-supervised spatiotemporal learning via video clip order prediction. In *IEEE/CVF Conference on Computer Vision and Pattern Recognition*, 2019.

Yan, W., Zhang, Y., Abbeel, P., and Srinivas, A. Videogpt: Video generation using VQ-VAE and transformers. *arXiv preprint arXiv:2104.10157*, 2021.

Yang, C., Xu, Y., Dai, B., and Zhou, B. Video representation learning with visual tempo consistency. *arXiv preprint arXiv:2006.15489*, 2020.

Yun, S., Han, D., Oh, S. J., Chun, S., Choe, J., and Yoo, Y. Cutmix: Regularization strategy to train strong classifiers with localizable features. In *IEEE/CVF International Conference on Computer Vision*, 2019.

Zhang, H., Cisse, M., Dauphin, Y. N., and Lopez-Paz, D. mixup: Beyond empirical risk minimization. *arXiv preprint arXiv:1710.09412*, 2017.

Zhang, Z. and Tao, D. Slow feature analysis for human action recognition. *IEEE Transactions on Pattern Analysis and Machine Intelligence*, 2012.

Zhou, D., Kang, B., Jin, X., Yang, L., Lian, X., Hou, Q., and Feng, J. Deepvit: Towards deeper vision transformer. *arXiv preprint arXiv:2103.11886*, 2021.

Zhou, J., Wei, C., Wang, H., Shen, W., Xie, C., Yuille, A., and Kong, T. ibot: Image bert pre-training with online tokenizer. *International Conference on Learning Representations (ICLR)*, 2022.

Appendix

This appendix provide more additional details of VideoMAE: § A contains the detailed architectures of VideoMAE. § B contains the implementation details of our proposed VideoMAE. § C contains the experiments on downstream action detection task and more detailed comparison with the state-of-the-art on the Something-Something V2, Kinetics-400, UCF101, HMDB51 and AVA datasets. § D contains several examples of reconstruction to further analyze our VideoMAE.

A. Architectures

We use an asymmetric encoder-decoder architecture for video self-supervised pre-training and discard the decoder during the fine-tuning phase. We take the 16-frame vanilla ViT-Base for example, and the specific architectural design for the encoder and decoder is shown in Table 8. We adopt the joint space-time attention (Arnab et al., 2021) to better capture the high-level spatio-temporal information in the remaining tokens.

Stage	Vision Transformer (Base)	Output Sizes
data	stride $4 \times 1 \times 1$ on K400 stride $2 \times 1 \times 1$ on SSV2	$3 \times 16 \times 224 \times 224$
cube	$2 \times 16 \times 16, 768$ stride $2 \times 16 \times 16$	$768 \times 8 \times 196$
mask	tube mask mask ratio = ρ	$768 \times 8 \times [196 \times (1-\rho)]$
encoder	MHA(768) MLP(3072) $\times 12$	$768 \times 8 \times [196 \times (1-\rho)]$
projector	MLP(384) & concat learnable tokens	$384 \times 8 \times 196$
decoder	MHA(384) MLP(1536) $\times 4$	$384 \times 8 \times 196$
projector	MLP(1536)	$1536 \times 8 \times 196$
reshape	from 1536 to $3 \times 2 \times 16 \times 16$	$3 \times 16 \times 224 \times 224$

Table 8. Architectures details of VideoMAE. We take 16-frame vanilla ViT-Base for example. ‘‘MHA’’ here denotes the joint space-time self-attention. The output sizes are denoted by $\{C \times T \times S\}$ for channel, temporal and spatial sizes. We use the asymmetric encoder-decoder architecture for video self-supervised pre-training and discard the decoder during the fine-tuning phase.

B. Implementation Details

We conduct the experiments with 64 Tesla V100 GPUs for both pre-training and fine-tuning on Something-Something V2 and Kinetics-400 datasets. The experiments on smaller UCF101 and HMDB51 are trained on 8 GPUs. We linearly scale the base learning rate w.r.t. the overall batch size, $lr = \text{base learning rate} \times \frac{\text{batch size}}{256}$. We adopt the PyTorch (Paszke et al., 2019) and DeepSpeed frameworks for faster training.

Something-Something V2. Our VideoMAE is pre-trained for 800 epochs on Something-Something V2 by default. During the fine-tuning phase, we perform the uniform sam-

config	Sth-Sth V2	Kinetics-400
optimizer	AdamW	
base learning rate	1.5e-4	
weight decay	0.05	
optimizer momentum	$\beta_1, \beta_2 = 0.9, 0.95$ (Chen et al., 2020a)	
batch size	1024(B), 512(L)	
learning rate schedule	cosine decay (Loshchilov & Hutter, 2016)	
warmup epochs	40	
flip augmentation	no	yes
augmentation	MultiScaleCrop	

Table 9. Pre-training setting.

config	Sth-Sth V2	Kinetics-400
optimizer	AdamW	
base learning rate	5e-4	1e-3
weight decay	0.05	
optimizer momentum	$\beta_1, \beta_2 = 0.9, 0.999$	
layer-wise lr decay	0.75 (Bao et al., 2021)	
batch size	512(B), 256(L)	
learning rate schedule	cosine decay	
warmup epochs	5	
training epochs	50	100(B), 60(L)
flip augmentation	no	yes
RandAug	(0, 0.5) (Cubuk et al., 2020)	
label smoothing	0.1 (Szegedy et al., 2016)	
mixup	0.8 (Zhang et al., 2017)	
cutmix	1.0 (Yun et al., 2019)	
drop path	0.1	

Table 10. End-to-end fine-tuning setting.

config	Sth-Sth V2
optimizer	SGD
base learning rate	0.1
weight decay	0
optimizer momentum	0.9
batch size	1024
learning rate schedule	cosine decay
warmup epochs	10
training epochs	100
augmentation	MultiScaleCrop

Table 11. Linear probing setting.

config	AVA
optimizer	AdamW
base learning rate	2.5e-4
weight decay	0.05
optimizer momentum	$\beta_1, \beta_2 = 0.9, 0.999$
layer-wise lr decay	0.75 (Bao et al., 2021)
batch size	128
learning rate schedule	cosine decay
warmup epochs	5
training epochs	30
flip augmentation	yes
drop path	0.2

Table 12. Fine-tuning setting on AVA 2.2.

pling following TSN (Wang et al., 2019). For evaluation, all models share the same inference protocol, i.e., 2 clips $\times 3$ crops. The default settings of pre-training, fine-tuning, and linear probing are shown in Table 9, Table 10, and Table 11. For supervised training, we follow the recipe in (Fan et al., 2021) and train from scratch for 100 epochs. Note that we use *no flip augmentation* during both the pre-training and fine-tuning phase. We additionally adopt the repeated augmentation (Hoffer et al., 2020) during the fine-tuning phase in Table 6 and Table 13, which can further increase the Top-1 accuracy by about 0.2%.

Kinetics-400. VideoMAE is pre-trained for 800 epochs on Kinetics-400 by default. During the fine-tuning phase, we perform the dense sampling following Slowfast (Feichtenhofer et al., 2019). For evaluation, all models share the same inference protocol, i.e., 5 clips \times 3 crops. The default settings of pre-training and fine-tuning are shown in Table 9 and Table 10. For supervised training from scratch, we follow the recipe in (Fan et al., 2021) and train the model for 200 epochs. Note that we additionally adopt the repeated augmentation (Hoffer et al., 2020) during the fine-tuning phase in Table 7 and Table 14, which can further increase the Top-1 accuracy by about 0.8%.

UCF101. We follow a similar recipe on Kinetics for pre-training. Our VideoMAE is pre-trained with a batch size of 192 for 3200 epochs. The base learning rate is set to 3e-4. Here, 16 frames with a temporal stride of 4 are sampled. For fine-tuning, the model is trained with a batch size of 128 for 100 epochs. The base learning rate is set to 1e-3.

HMDB51. Our VideoMAE is pre-trained with a batch size of 192 for 4800 epochs. The base learning rate is set to 3e-4. Here, 16 frames with a temporal stride of 2 are sampled. For fine-tuning, the model is trained with a batch size of 128 for 60 epochs. The base learning rate is set to 1e-3.

AVA. We follow the action detection architecture in Slowfast (Feichtenhofer et al., 2019) and use the detected person boxes from AIA (Tang et al., 2020). The default settings of fine-tuning are shown in Table 12. For data augmentations, we resize the short side of the input frames to 256 pixels. We apply a random crop of the input frames to 224×224 pixels and random flip during training. We use only ground-truth person boxes for training and the detected boxes with confidence ≥ 0.8 for inference.

C. Additional Results

C.1. Training schedule

Figure 7 shows the influence of the longer pre-training schedule on the Something-Something V2 and Kinetics-400 datasets. We find that a longer pre-training schedule brings slight gains to both datasets. In the main paper, our VideoMAE is pre-trained for 800 epochs by default.

C.2. Comparison with the state of the art

Table 13 shows more detailed comparison with the state of the art on Something-Something V2, and Table 14 presents more detailed comparison with the results on Kinetics-400. We present the detailed comparison with the state of the art on UCF101 and HMDB51 in Table 15.

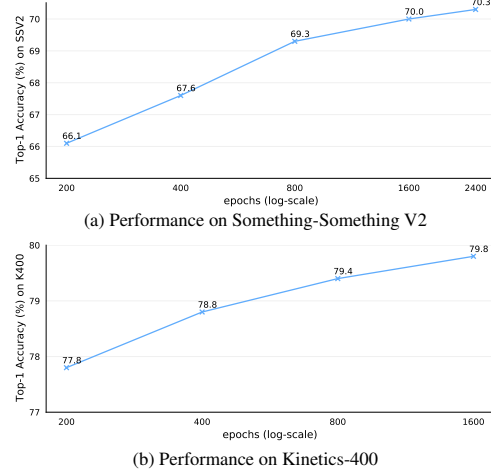


Figure 7. The effect of **training schedules** on (a) Something-Something V2 and (b) Kinetics-400. Here each point is a full training schedule. Our default ViT-B backbone is described in Appendix A.

D. Additional Visualization Examples

We show several examples of reconstruction in Figure 8 and Figure 9. Videos are all chosen from the validation set.

Method	Backbone	Extra data	Extra labels	Frames	GFLOPs	Param	Top-1	Top-5
TSM _{two stream} (Lin et al., 2019)	ResNet50×2	ImageNet-1K	✓	16+16	130×2×3	49	66.0	90.5
TEINet _{En} (Liu et al., 2020)	ResNet50×2		✓	8+16	99×10×3	50	66.6	N/A
TANet _{En} (Liu et al., 2021c)	ResNet50×2		✓	8+16	99×2×3	51	66.0	90.1
TDN _{En} (Wang et al., 2021a)	ResNet101×2		✓	8+16	198×1×3	88	69.6	92.2
SlowFast (Feichtenhofer et al., 2019)	ResNet101	Kinetics-400	✓	8+32	106×1×3	53	63.1	87.6
MViTv1 (Fan et al., 2021)	MViTv1-B		✓	64	455×1×3	37	67.7	90.9
MViTv1 (Fan et al., 2021)	MViTv1-B	Kinetics-600	✓	32	170×1×3	37	67.8	91.3
MViTv1 (Fan et al., 2021)	MViTv1-B-24		✓	32	236×1×3	53	68.7	91.5
TimeSformer (Bertasius et al., 2021)	ViT-B	ImageNet-21K	✓	8	196×1×3	121	59.5	N/A
TimeSformer (Bertasius et al., 2021)	ViT-L		✓	64	5549×1×3	430	62.4	N/A
ViViT FE (Arnab et al., 2021)	ViT-L	IN-21K+K400	✓	32	995×4×3	N/A	65.9	89.9
Motionformer (Patrick et al., 2021b)	ViT-B		✓	16	370×1×3	109	66.5	90.1
Motionformer (Patrick et al., 2021b)	ViT-L		✓	32	1185×1×3	382	68.1	91.2
Video Swin (Liu et al., 2021b)	Swin-B		✓	32	321×1×3	88	69.6	92.7
VIMPAC (Tan et al., 2021)	ViT-L	HowTo100M+DALLE	✗	10	N/A×10×3	307	68.1	N/A
BEVT-V (Wang et al., 2021b)	Swin-B		✗	32	321×1×3	88	67.1	N/A
BEVT (Wang et al., 2021b)	Swin-B		✗	32	321×1×3	88	70.6	N/A
MaskFeat \uparrow 312 (Wei et al., 2021)	MViT-L		✓	40	2828×1×3	218	74.4	94.6
MaskFeat \uparrow 312 (Wei et al., 2021)	MViT-L		✓	40	2828×1×3	218	75.0	95.0
VideoMAE $_{\rho=90\%}$ (Ours)	ViT-B	no external data	✗	16	180×2×3	87	70.6	92.7
VideoMAE $_{\rho=90\%}$ (Ours)	ViT-L		✗	16	597×2×3	305	74.2	94.7
VideoMAE $_{\rho=90\%}$ (Ours)	ViT-L		✗	32	1436×1×3	305	75.3	95.2

Table 13. Comparison with the state-of-the-art methods on Something-Something V2. Here our VideoMAE reconstructs normalized cube pixels and is pre-trained with *mask ratio* $\rho=90\%$ for 2400 epochs. The GFLOPs of a single view \times the number of views (temporal clips with spatial crops) represents the model complexity. “N/A” indicates the numbers are not available for us.

Method	Backbone	Extra data	Extra labels	Frames	GFLOPs	Param	Top-1	Top-5
NL I3D (Wang et al., 2018)	ResNet101	ImageNet-1K	✓	128	359×10×3	62	77.3	93.3
TANet (Liu et al., 2021c)	ResNet152		✓	16	242×4×3	59	79.3	94.1
TDN _{En} (Wang et al., 2021a)	ResNet101×2		✓	8+16	198×10×3	88	79.4	94.4
Video Swin (Liu et al., 2021b)	Swin-B		✓	32	282×4×3	88	80.6	94.6
TimeSformer (Bertasius et al., 2021)	ViT-B	ImageNet-21K	✓	8	196×1×3	121	78.3	93.7
TimeSformer (Bertasius et al., 2021)	ViT-L		✓	96	8353×1×3	430	80.7	94.7
ViViT FE (Arnab et al., 2021)	ViT-L		✓	128	3980×1×3	N/A	81.7	93.8
Motionformer (Patrick et al., 2021b)	ViT-B		✓	16	370×10×3	109	79.7	94.2
Motionformer (Patrick et al., 2021b)	ViT-L		✓	32	1185×10×3	382	80.2	94.8
Video Swin (Liu et al., 2021b)	Swin-B		✓	32	282×4×3	88	82.7	95.5
Video Swin (Liu et al., 2021b)	Swin-L		✓	32	604×4×3	197	83.1	95.9
ip-CSN (Ghadiyaram et al., 2019)	ResNet152	IG-65M	✓	32	109×10×3	33	82.5	95.3
CorrNet (Wang et al., 2020a)	ResNet101		✓	32	224×10×3	N/A	81.0	N/A
ViViT FE (Arnab et al., 2021)	ViT-L		✓	128	3980×1×3	N/A	83.5	94.3
ViViT (Arnab et al., 2021)	ViT-H		✓	32	3981×4×3	N/A	84.9	95.8
VIMPAC (Tan et al., 2021)	ViT-L		✗	10	N/A×10×3	307	77.4	N/A
BEVT-V (Wang et al., 2021b)	Swin-B		✗	32	282×4×3	88	76.2	N/A
BEVT (Wang et al., 2021b)	Swin-B		✗	32	282×4×3	88	80.6	N/A
MaskFeat \uparrow 352 (Wei et al., 2021)	MViT-L	Kinetics-600	✗	40	3790×4×3	218	87.0	97.4
ip-CSN (Tran et al., 2019)	ResNet152		✗	32	109×10×3	33	77.8	92.8
SlowFast (Feichtenhofer et al., 2019)	R101+NL		✗	16+64	234×10×3	60	79.8	93.9
CorrNet (Wang et al., 2020a)	ResNet101		✗	32	224×10×3	N/A	79.2	N/A
X3D (Feichtenhofer, 2020)	X3D-XL	no external data	✗	16	48×10×3	11	79.1	93.9
MoViNet (Kondratyuk et al., 2021)	MoViNet-A6		✗	120	386×1×1	31	81.5	95.3
MViTv1 (Fan et al., 2021)	MViTv1-B		✗	32	170×5×1	37	80.2	94.4
MViTv1 (Fan et al., 2021)	MViTv1-B		✗	64	455×3×3	37	81.2	95.1
MaskFeat (Wei et al., 2021)	MViT-L	Kinetics-600	✗	16	377×10×1	218	84.3	96.3
VideoMAE $_{\rho=90\%}$ (Ours)	ViT-B		✗	16	180×5×3	87	80.9	94.7
VideoMAE $_{\rho=90\%}$ (Ours)	ViT-L		✗	16	597×5×3	305	84.7	96.5
VideoMAE $_{\uparrow320\rho=90\%}$ (Ours)	ViT-L		✗	32	3958×5×3	305	85.8	97.1

Table 14. Comparison with the state-of-the-art methods on Kinetics-400. Our VideoMAE reconstructs normalized cube pixels. Here models are pre-trained for 1600 epochs on Kinetics-400. The GFLOPs of a single view \times the number of views (temporal clips with spatial crops) represents the model complexity. “N/A” indicates the numbers are not available for us.

Method	Backbone	Extra data	Frames	Param	Modality	UCF101	HMDB51
OPN (Lee et al., 2017)	VGG	UCF101	N/A	N/A	V	59.6	23.8
VCOP (Xu et al., 2019)	R(2+1)D	UCF101	N/A	N/A	V	72.4	30.9
CoCLR (Han et al., 2020a)	S3D-G	UCF101	32	9M	V	81.4	52.1
Vi ² CLR (Diba et al., 2021)	S3D	UCF101	32	9M	V	82.8	52.9
VideoMAE(Ours)	ViT-B	<i>no external data</i>	16	87M	V	90.8	61.1
SpeedNet (Benaim et al., 2020)	S3D-G	Kinetics-400	64	9M	V	81.1	48.8
VTHCL (Yang et al., 2020)	SlowOnly-R50	Kinetics-400	8	32M	V	82.1	49.2
Pace (Wang et al., 2020b)	R(2+1)D	Kinetics-400	16	15M	V	77.1	36.6
MemDPC (Han et al., 2020b)	R-2D3D	Kinetics-400	40	32M	V	86.1	54.5
CoCLR (Han et al., 2020a)	S3D-G	Kinetics-400	32	9M	V	87.9	54.6
RSPNet (Chen et al., 2021a)	S3D-G	Kinetics-400	64	9M	V	93.7	64.7
VideoMoCo (Pan et al., 2021b)	R(2+1)D	Kinetics-400	16	15M	V	78.7	49.2
Vi ² CLR (Diba et al., 2021)	S3D	Kinetics-400	32	9M	V	89.1	55.7
CVRL (Qian et al., 2021b)	SlowOnly-R50	Kinetics-400	32	32M	V	92.9	67.9
CVRL (Qian et al., 2021b)	SlowOnly-R50	Kinetics-600	32	32M	V	93.6	69.4
CVRL (Qian et al., 2021b)	Slow-R152 (2 \times)	Kinetics-600	32	328M	V	94.4	70.6
CORP _f (Hu et al., 2021)	SlowOnly-R50	Kinetics-400	32	32M	V	93.5	68.0
ρ SimCLR($\rho=2$) (Feichtenhofer et al., 2021)	SlowOnly-R50	Kinetics-400	8	32M	V	88.9	N/A
ρ SwAV($\rho=2$) (Feichtenhofer et al., 2021)	SlowOnly-R50	Kinetics-400	8	32M	V	87.3	N/A
ρ MoCo($\rho=2$) (Feichtenhofer et al., 2021)	SlowOnly-R50	Kinetics-400	8	32M	V	91.0	N/A
ρ BYOL($\rho=2$) (Feichtenhofer et al., 2021)	SlowOnly-R50	Kinetics-400	8	32M	V	92.7	N/A
ρ BYOL($\rho=4$) (Feichtenhofer et al., 2021)	SlowOnly-R50	Kinetics-400	8	32M	V	94.2	72.1
MIL-NCE (Miech et al., 2020)	S3D	HowTo100M	32	9M	V+T	91.3	61.0
MMV (Alayrac et al., 2020)	S3D-G	AS+HTM	32	9M	V+A+T	92.5	69.6
ELO (Piergiovanni et al., 2020)	R(2+1)D	Youtube8M-2	N/A	N/A	V+A	93.8	67.4
XDC (Alwassel et al., 2020)	R(2+1)D	Kinetics-400	32	15M	V+A	84.2	47.1
XDC (Alwassel et al., 2020)	R(2+1)D	IG65M	32	15M	V+A	94.2	67.1
GDT (Patrick et al., 2021a)	R(2+1)D	Kinetics-400	32	15M	V+A	89.3	60.0
GDT (Patrick et al., 2021a)	R(2+1)D	IG65M	32	15M	V+A	95.2	72.8
VideoMAE(Ours)	ViT-B	Kinetics-400	16	87M	V	96.1	73.3

Table 15. Comparison with the state-of-the-art methods on UCF101 and HMDB51. We report fine-tuning accuracy for evaluation. ‘V’ refers to visual only, ‘A’ is audio, ‘T’ is text narration. “N/A” indicates the numbers are not available for us.

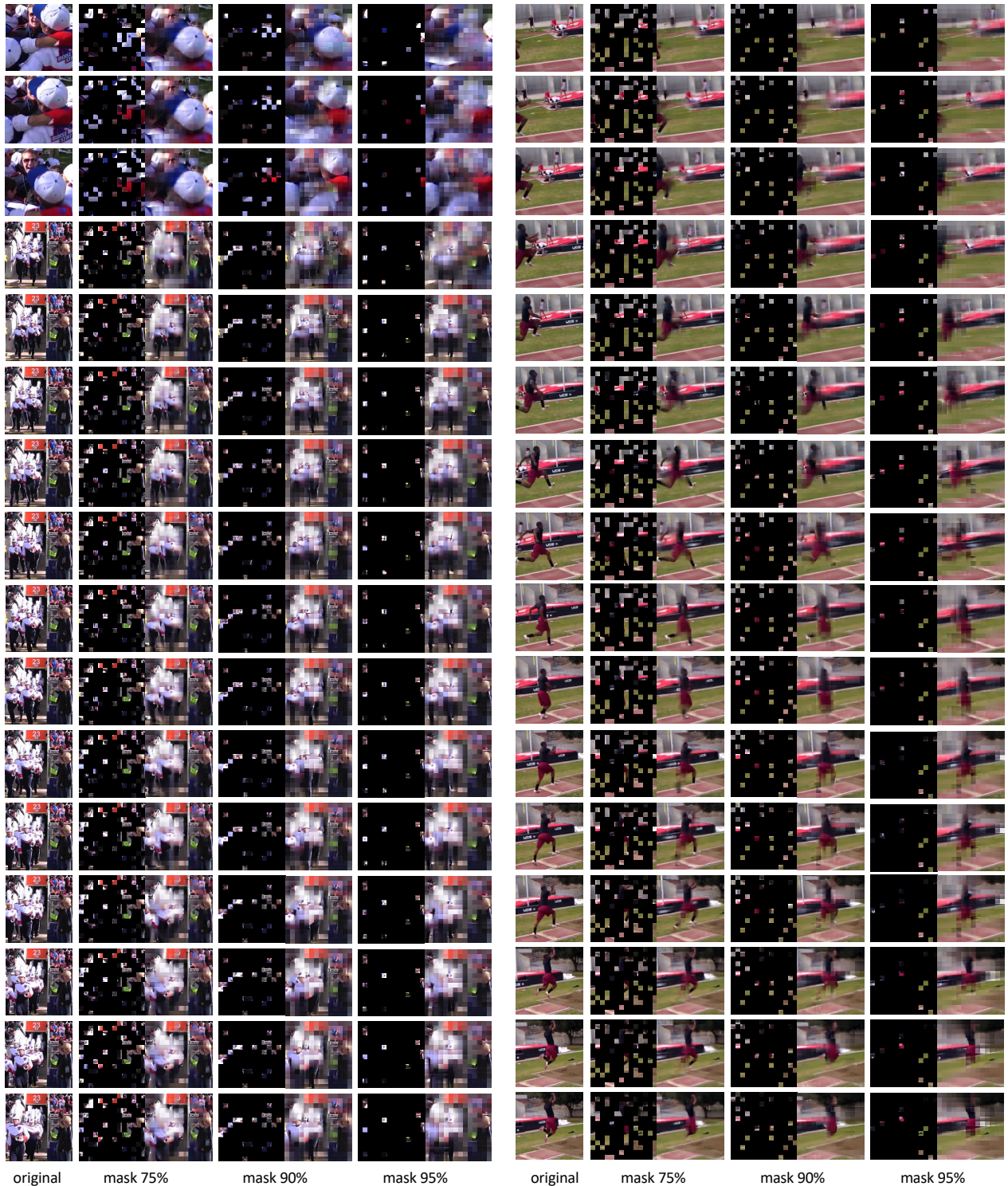


Figure 8. Uncurated random videos on Kinetics-400 validation set. We show the original video sequence and reconstructions with different masking ratios. Reconstructions of videos are predicted by our VideoMAE pre-trained with a masking ratio of 90%.

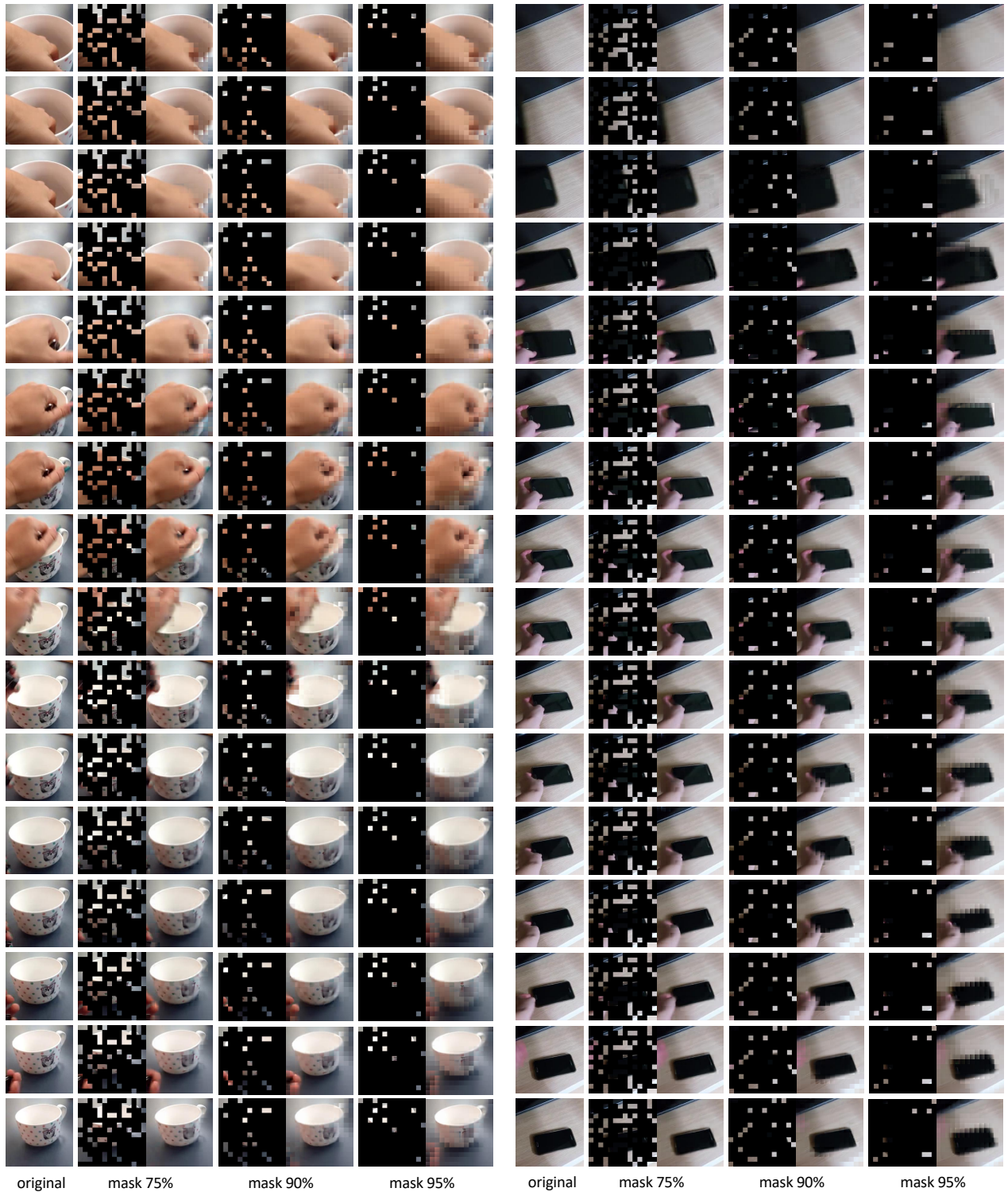


Figure 9. **Uncurated random videos** on Something-Something V2 *validation* set. We show the original video sequence and reconstructions with different masking ratios. Reconstructions of videos are all predicted by our VideoMAE pre-trained with a masking ratio of 90%.